Electronic Supplementary Material (ESI) for Environmental Science: Nano.

Electronic Supplementary Files

Fluorescent labelled SiO_2 nanoparticles as tracers in natural waters. Dependence of detection limits with environmental conditions

Alberto Clemente, Nuria Moreno, M. Pilar Lobera, Francisco Balas and Jesus Santamaria

1. Estimation of the limits of detection

The detection decision for a net fluorescence signal (S) at a given wavelength (*i.e.* the critical level, S_C) and the detection limit in the same conditions (*i.e.* the minimum detectable value, S_D) have been defined as the following probabilities:

$$p\left(\hat{S} > S_C \,\middle|\, S = 0\right) \leq \alpha$$

$$p\left(\hat{S} \leq S_C \,\middle|\, S = S_D\right) = \beta$$

where the inequality in the probability distribution function of the critical level resulted because not all values of α (probability of false positives) were possible for discrete distributions. Assuming that the probability distributions of signals (S) were normal with constant standard deviation (homoscedasticity), the previous equations led to the expressions:

$$S_C = z_{1-\alpha}\sigma_o$$

$$S_D = S_C + z_{1-\beta}\sigma_o$$

where σ_o is the standard deviation of $\hat{S}$ when S = 0 and $z_{1-\alpha}$ and $z_{1-\beta}$ are the percentiles of the one-tailed normal distributions under the null (H_0: absent analyte) and alternative hypothesis (H_a: analyte present at minimum detectable value) with significance levels α and β respectively. In the simplest case of homoscedasticity and assuming that α = β, the minimum detectable signal, S_D, can be estimated as:

$$S_D = 2z_{1-\alpha}\sigma_o$$

The application to the concentration domain requires the knowledge of the distribution of the concentration estimator (ĉ) for transforming the observed net signal (S) into the concentration (c) values. For the simplest calibration function, a straight line obtained from single-component regression analysis with normal distribution of the response (y), the estimation of the concentration can be calculated from the estimation of the net signal (S) and the estimation of the sensitivity (*i.e.* the slope of the regression curve, A) of the test. Formally, it can be expressed as:

$$\hat{c} = \frac{\hat{S}}{\hat{A}} = \frac{y - \hat{B}}{\hat{A}}$$

Both sensitivity (A) and zero intercept (B) were calculated through calibration of the fluorescence intensity signal (y) *vs.* concentration (c) using ordinary least squares regression. The expression for the concentration detection limit (c_D) was immediately obtained from the expression of the minimum detectable value of the net fluorescence signal (S_D) as:

$$c_D = \frac{S_D}{A} = \frac{2z_{1-\alpha}\sigma_o}{A}$$

This is correct for normally distributed data with constant and known variance and with α = β. The estimation of σ_o was another important parameter to be determined. Taking into account the variance (σ^2) propagation, based on the definition of the estimated net signal, it can be found that the estimation of the variance of net fluorescence signals can be calculated as:

$$\sigma^2_{\hat{S}} = \sigma^2_y + \sigma^2_{\hat{B}}$$

The variance of $\hat{S}$ when S = 0 (σ_o^2) is therefore:

$$\sigma_o^2 = \sigma_B^2 + \sigma_{\hat{B}}^2 = \left(1 + \frac{\sigma_{\hat{B}}^2}{\sigma_B^2}\right)\sigma_B^2 = \eta\sigma_B^2$$

If the variance of the estimator $\hat{B}$ is negligible, then $\sigma_o = \sigma_B$ that is the standard deviation of the measured blank. The design parameter η reflects the relative number of replicates and for calibration-based experiments, this parameter takes into account the distribution of every concentration *vs.* signal intensity standards and the calibration structure (*i.e.* the number of calibration points, replicates, etc.). When referring to ordinary least-squares regression, the value of η is estimated as:

$$\eta = 1 + \frac{1}{kn} + \frac{\bar{c}_w^2}{S_{ccw}}$$

for **n** calibration points consisting in **k** replicates. The term S_{ccw} is the weighted sum of squared deviations of every calibration point from $\bar{c}_w$, the weighted mean concentration. The weights were estimated as the inverse variance (σ_c^2) of every calibration point.

The values of the detection limits can be effectively determined using the calibration data of the intensity of the fluorescence signal at the emission wavelength. The dependence of the signal intensity (y) with the concentration (c) is obtained by ordinary least squares regression analysis on the obtained data.

$$c_D = \frac{2z_{1-\alpha}\sqrt{\eta}}{A}\sigma_B$$

Since the calculation of the variance of the blank measurements (σ_B^2) was done after a k = 10 replicates, it would be more adequate to assume instead the standard deviation of the sample (s_B). In such case, the value of the percentile $z_{1-\alpha}$ of the normal distribution was changed for the percentile of the one-tailed Student-t distribution with confidence level (1-α) and ν = k-2 degrees of freedom ($t_{1-\alpha,\nu}$):

$$c_D = \frac{2t_{1-\alpha,\nu}\sqrt{\eta}}{A} s_B$$

In the present study, a total of n = 10 calibration points were chosen, with k = 10 replicates for every calibration point and a confidence level of (1-α) = 0.95 was selected. The final expression for calculating the values of c_D was:

$$c_D = \frac{(3.719)s_B}{A}$$

2. Calibration data

Fluorescent-labelled nanoparticles were dispersed in the different media at a starting concentration of 10 ppm, which was sequentially diluted down to 5 ppm, 1 ppm, 500 ppb, 100 ppb, 50 ppb, 10 ppb, 5 ppb and 1 ppb. Blank spectra were recorded using milli-Q water in the same conditions as described for labelled nanoparticles in the dispersion media. Spectra of the suspended samples were sequentially recorded in the fluorescence spectrometer at the above-cited excitation and emission wavelength for every labelled material. Samples were dispersed in three similar flasks at the same concentration and every sample was measured three times in the fluorescence spectrometer. This measurement scheme provided nine values of fluorescence intensity per sample and nanoparticle concentration and per dispersion media. Intensity of the emission peak at every testing wavelength was then plotted against the concentration in every dispersion media. Data were then fitted using linear regression ($I = A \cdot c + B$; with A = slope and B = zero intercept) by using an ordinary least squares scheme. Fitting parameters were calculated with a 95% of confidence level ($\alpha = 0.05$). In Table S1 and Figure S1 are shown the calibration results for $Ru(phen)_3$:SiO_2 nanoparticles in the different aquatic environment.

Table S1. Calibration data for fluorescence emission at 448 nm of suspended $Ru(phen)_3$:SiO_2 nanoparticles in different aquatic media during different immersion periods (data were fitted using an ordinary least-squares algorithm)

t = 0 days	Slope	Intercept	SE Blank	R^2
Milli-Q	0.0161	4.063	0.156	0.999851
Tap Water	0.0104	9.089	0.185	0.997070
SiO_2 10 ppm	0.0157	8.530	0.193	0.999940
Canal	0.0053	24.378	0.323	0.994373
Seawater	0.0081	4.534	0.161	0.999922

t = 1 day	Slope	Intercept	SE Blank	R^2
Milli-Q	0.0108	2.684	0.147	0.998176
Tap Water	0.0074	8.335	0.124	0.999228
SiO_2 10 ppm	0.0105	6.708	0.136	0.999307
Canal	0.0046	15.607	0.457	0.970377
Seawater	0.0081	4.457	0.165	0.999854

t = 2 days	Slope	Intercept	SE Blank	R^2
Milli-Q	0.0102	0.809	0.151	0.997989
Tap Water	0.0074	6.469	0.187	0.998565
SiO_2 10 ppm	0.0101	6.664	0.114	0.999271
Canal	0.0045	14.772	0.184	0.969251
Seawater	0.0082	4.452	0.088	0.999954

t = 8 days	Slope	Intercept	SE Blank	R^2
Milli-Q	0.0062	11.975	0.147	0.980258
Tap Water	0.0071	5.291	0.186	0.999646
SiO_2 10 ppm	0.0066	15.231	0.162	0.979929
Canal	0.0052	10.713	0.456	0.980462
Seawater	0.0085	4.462	0.136	0.999981

t = 210 days	Slope	Intercept	SE Blank	R^2
Milli-Q	0.0045	9.658	0.068	0.967663
Tap Water	0.0070	5.472	0.076	0.999641
SiO_2 10 ppm	0.0045	12.906	0.171	0.897333
Canal	0.0038	13.884	1.004	0.962600
Seawater	0.0080	4.167	0.114	0.999859

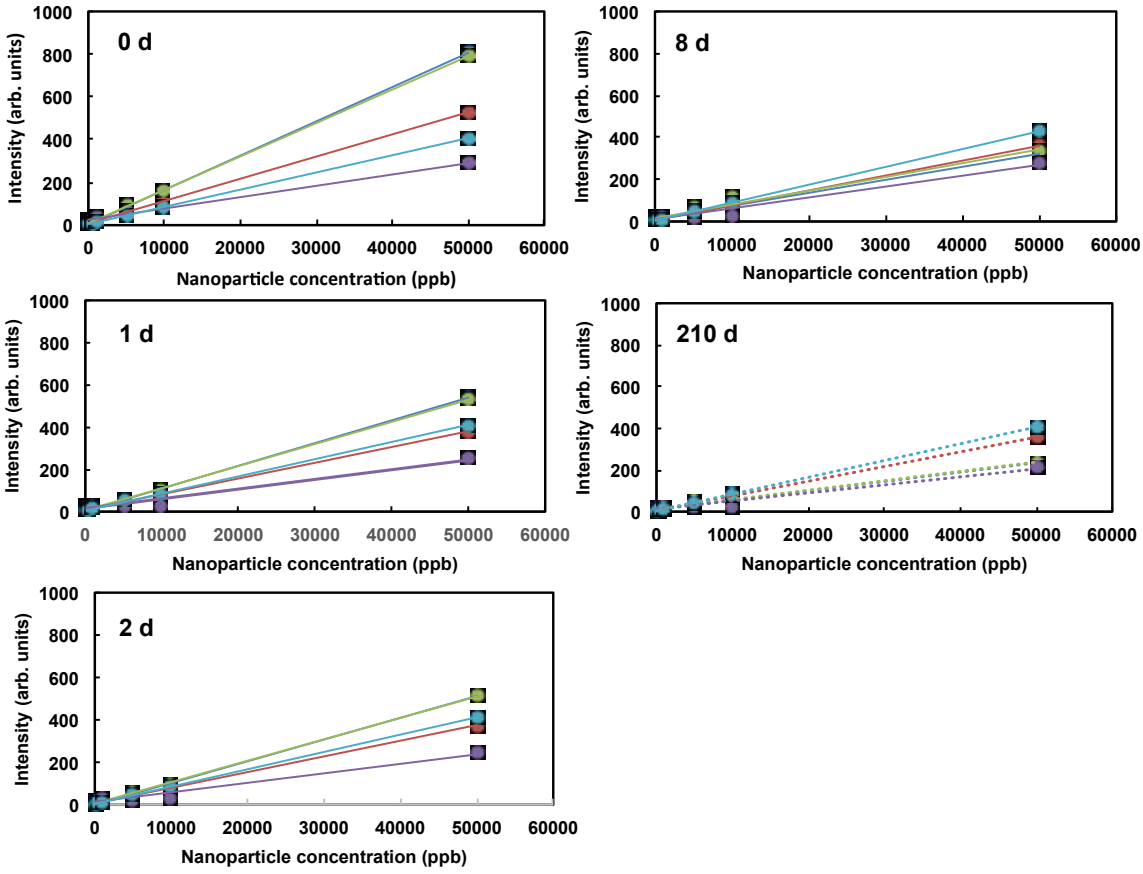

Figure S1. Calibration curves of $Ru(phen)_3$:SiO_2 nanoparticles in different aquatic environments upon stabilization (t = 0d) and after several periods of storage

In addition, the stability of labelled nanoparticles in the tested aqueous environments at different concentrations was analysed. Figure S2 shows the temporal evolution of the relative emission intensity ($I(t_e)/I_0$) as function of the elapsed time of immersion in the aqueous media. As it can be observed, the emission intensity decayed about of 60% of the original intensity when the storage time was over 48 h, remaining almost constant for all testing media even after 210 d in the water. This fact was similar for concentrations from 1 ppm to 50 ppm of labelled nanoparticles in every environment.

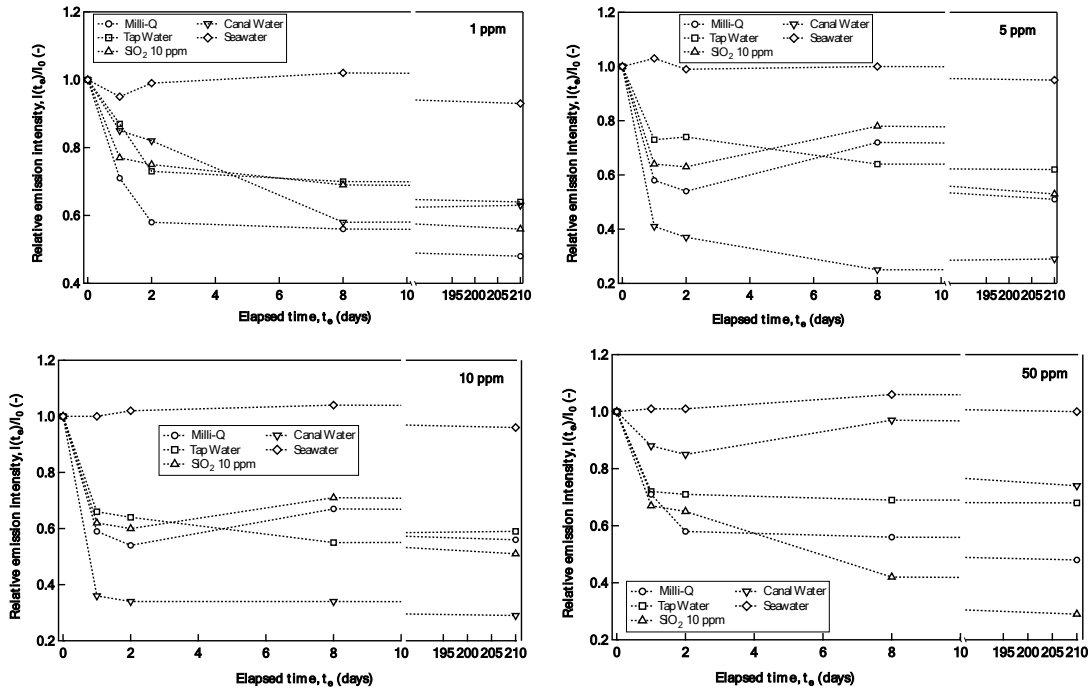

Figure S2. Time evolution of the fluorescence emission intensity of aqueous suspensions at different concentrations of $Ru(phen)_3$:SiO_2 nanoparticles in different aquatic environments upon stabilization (t = 0d) and after several periods of storage

3. X-ray photoelectron spectroscopy data of $Ru(phen)_3$:SiO_2

The presence of ruthenium in the reddish $Ru(phen)_3$:SiO_2 nanoparticles was analysed using X-ray photoelectron spectroscopy (Figure S3) in a Kratos AXIS Ultra DLD system with a monochromatized Al Kα beam at 1466 eV.

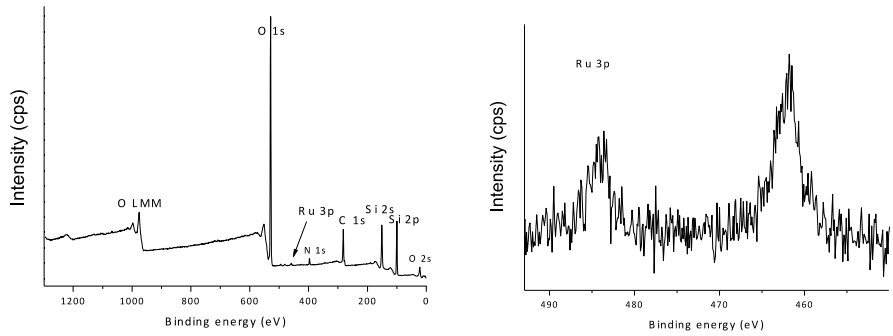

Figure S3. Survey-scan and Ru3d XPS spectra of the $Ru(phen)_3$:SiO_2 nanoparticles

The analysis of the XPS data (Table S2) showed that the relative content of Ru in the surface of $Ru(phen)_3$:SiO_2 nanoparticles was about 0.4%.

Table S2. XPS data of $Ru(phen)_3:SiO_2$ nanoparticles

Peak	Binding energy (eV)	Atomic (%)
C 1s	284.9	20.14
O 1s	532.4	55.71
Si 2p	103.1	23.74
Ru 3p	461.8	0.41

4. Scanning electron microscopy images $Ru(phen)_3:SiO_2$

The homogeneity in particle sizes of the fluorescent-labelled nanoparticles could be also confirmed after the SEM images (Figure S4) taken using a FEI-F Inspect field-emission microscope.

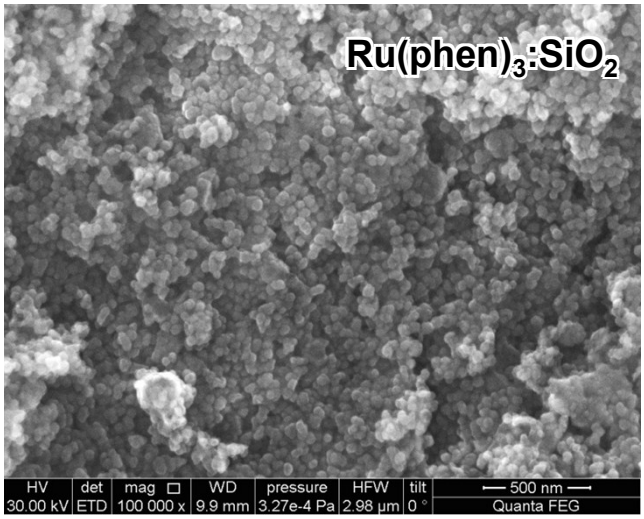

Figure S4. SEM images of $Ru(phen)_3:SiO_2$ nanoparticles